# Supporting Information

## Devanapally et al. 10.1073/pnas.1423333112

### SI Materials and Methods

**Strains Used.** N2 wild type, AMJ2 *eri-1*(*mg366*) *nrIs20* (*Psur-5::sur-5::gfp*) *IV*; *sid-1*(*qt9*) *V*; *qtIs49* (*Prgef-1::gfp–dsRNA* and *pRF4*) *III*, AMJ154 *eri-1*(*mg366*) *nrIs20 IV*; *qtIs49 III*, AMJ265 *rrf-1*(*ok589*) *I*; *oxSi487* [*Pmex-5::gfp* and *unc-119*(+)] *II*; *unc-119*(*ed3*)*? III*, AMJ300 *nrIs20 IV*; *qtIs49 III*, AMJ301 *qtIs49 III*, AMJ310 *eri-1*(*mg366*) *nrIs20 IV*; *mIs10* (*Pmyo-2::gfp*) *V*, AMJ320 *nrIs20 IV*; *sid-1*(*qt9*) *V*; *qtIs49 III*, AMJ324 *oxSi487 II*; *unc-119*(*ed3*)*? III*; *sid-1*(*qt9*) *V* (generated by Julia Marré, A.M.J. laboratory, University of Maryland, College Park, MD), AMJ326 *oxSi487 II*; *unc-119*(*ed3*)*? III*; *rde-1*(*ne219*) *V* (generated by Julia Marré), AMJ349 *oxSi221* [*Peft-3::gfp* and *unc-119*(+)] *II*; *unc-119*(*ed3*)*? qtIs49 III*, AMJ361 *oxSi221 II*; *unc-119*(*ed3*)*? qtIs49 III*; *eri-1*(*mg366*) *IV*, AMJ363 *oxSi221 II*; *unc-119*(*ed3*)*? qtIs49 III*; *eri-1*(*mg366*) *IV*; *sid-1*(*qt9*) *V*, AMJ377 *oxSi487 II*; *unc-119*(*ed3*)*? III*; *eri-1*(*mg366*) *IV*, AMJ382 *oxSi221 II*; *unc-119*(*ed3*)*? III*; *eri-1*(*mg366*) *IV*, AMJ463 *oxSi487 II*; *unc-119*(*ed3*) *III ?*; *sid-1*(*qt9*) *V*; *jamEx131* (*pHC337* and *pHC448*), AMJ466 *oxSi487 II*; *unc-119*(*ed3*) *III*; *jamEx132* (*pHC337* and *pHC448*), AMJ502 *oxSi487 II*; *unc-119*(*ed3*) *III*; *jamEx145* (*pHC448*), AMJ471 *jamEx140* (*pHC337* and *pHC448*), AMJ533 *rde-1*(*ne219*) *V*; *jamEx140*, AMJ542 *sid-1*(*qt9*) *V*; *jamEx140*, AMJ577 *hrde-1*(*tm1200*) *III* [*4× outcrossed*], AMJ581 *oxSi487 dpy-2*(*e8*) *II*; *unc-119*(*ed3*)*? III* (generated by Samual Allgood, A.M.J. laboratory, University of Maryland, College Park, MD), AMJ585 *mut-7*(*ne4255*) *III* [*1× outcrossed*], AMJ586 *ox-Si487 dpy-2*(*e8*) *II*; *unc-119*(*ed3*)*? III*; *rde-1*(*ne219*) *V*, AMJ592 *hrde-1*(*tm1200*) *III*; *jamEx140*, AMJ593 *oxSi487 dpy-2*(*e8*) *II*; *unc-119*(*ed3*)*? III*; *sid-1*(*qt9*) *V*, AMJ595 *oxSi221 II*; *unc-119*(*ed3*)*? qtIs49 III*; *sid-1*(*qt9*) *V*, AMJ598 *oxSi487 dpy-2*(*e8*) *II*; *unc-119*(*ed3*)*? III*; *sid-1*(*qt9*) *V*; *jamEx140*, AMJ599 *oxSi487 dpy-2*(*e8*) *II*; *unc-119*(*ed3*)*? III*; *rde-1*(*ne219*) *V*; *jamEx140*, AMJ600 *ox-Si487 dpy-2*(*e8*) *II*; *unc-119*(*ed3*)*? III*; *jamEx140*, AMJ601 *oxSi487 dpy*(*e8*) *II*; *unc-119*(*ed3*)*? mut-7*(*ne4255*) *III*, AMJ602 *oxSi487 dpy-2*(*e8*) *II*; *unc-119*(*ed3*)*? hrde-1*(*tm1200*) *III*, AMJ603 *oxSi487 dpy-2*(*e8*) *II*; *unc-119*(*ed3*)*? III*; *qtEx136* (*Prgef-1::unc-22 dsRNA*) (1), AMJ620 *oxSi487 dpy-2*(*e8*) *II*; *unc-119*(*ed3*)*? hrde-1*(*tm1200*) *III*; *jamEx140 isolate 1*, AMJ621 *oxSi487 dpy-2*(*e8*) *II*; *unc-119*(*ed3*)*? hrde-1* (*tm1200*) *III*; *jamEx140 isolate 2*, AMJ628 *oxSi487 dpy-2*(*e8*) *II*; *unc-119*(*ed3*) *III?*; *jamEx147* (*pHC448*), AMJ639 *mut-7*(*ne4255*) *III*; *jamEx140*, AMJ643 *oxSi487 dpy-2*(*e8*) *II*; *unc-119*(*ed3*)*? mut-7*(*ne4255*) *III*; *jamEx140*, AMJ645 *oxSi487 dpy-2*(*e8*) *II*; *unc-119*(*ed3*)*? III*; *eri-1*(−) *IV*; *qtEx136*, EG6070 *oxSi221 II*; *unc-119*(*ed3*) *III*, EG6787 *oxSi487 II*; *unc-119*(*ed3*) *III*, GR1373 *eri-1*(*mg366*) *IV*, HC195 *nrIs20 IV*, HC196 *sid-1*(*qt9*) *V*, HC566 *nrIs20 IV*; *sid-1*(*qt9*) *V*, HC567 *eri-1*(*mg366*) *nrIs20 IV*, HC568 *eri-1*(*mg366*) *nrIs20 IV*; *sid-1*(*qt9*) *V*, HC780 *rrf-1*(*ok589*) *I* [*2× outcrossed*], and WM27 *rde-1*(*ne219*). The term dsRNA is used to refer to any form of base-paired RNA including hairpin RNA and double-stranded RNA for simplicity.

**Transgenic Animals.** Recombinant DNA fragments generated through overlap extension PCR using Expand Long Template polymerase (Roche) were purified by using the QIAquick PCR Purification Kit (Qiagen). Plasmids were purified by using the Plasmid mini kit (Qiagen). PCR products or plasmids were combined with a co-injection marker to transform *C. elegans* by using microinjection (2).

The plasmid pHC448 was used as a co-injection marker to express DsRed2 in the pharynx (1); pRF4 was used as a co-injection marker to express *rol-6(su1006)* (2); and pHC337 was used to express an inverted repeat of *gfp* in neurons (3), which is expected to generate a hairpin RNA (designated as *gfp–dsRNA*).

To express *gfp–dsRNA* in the neurons (*Prgef-1::gfp–dsRNA*): A 1:1 mixture of pHC337 (40 ng/μL) and pHC448 (40 ng/μL) in 10 mM Tris·HCl (pH 8.5) was microinjected into the wild-type strain N2 or into strains that express a single copy of *Pmex-5::gfp* in the germline as part of an operon (4) in wild-type [EG6787], *sid-1(−)* [AMJ324], *rde-1(−)* [AMJ326], *rrf-1(−)* [AMJ265], or *eri-1(−)* [AMJ377] backgrounds to generate three independent transgenic lines for each genetic background. In addition, pHC448 (40 ng/μL) in 10 mM Tris·HCl (pH 8.5) was injected into N2, EG6787, or AMJ377 to generate "no dsRNA" control transgenic lines.

**Balancing *sid-1*.** A transgene integrated on chromosome V [*mIs10* (*Pmyo-2::gfp*)] was used to balance *sid-1(qt9) V*. In Figs. 4*E* and S9, progeny of heterozygous *sid-1(qt9)/mIs10* animals were scored as homozygous mutants if they lacked GFP expression from *mIs10*. Tests using *rde-1* (~4.9 Mb from *sid-1*) suggest a low rate of recombination between *sid-1* and *mIs10*. Specifically, among the progeny of *rde-1(−)/mIs10* heterozygotes that lacked GFP expression from *mIs10*, ~94% (63/67) were found to be homozygous *rde-1(−)* by Sanger sequencing (determined by Edward Traver, A.M.J. laboratory, University of Maryland, College Park, MD).

**Genotyping *Prgef-1::gfp–dsRNA*.** The integrated transgene *qtIs49* was identified based on the cosegregation of the dominant Rol defect due to the pRF4 co-injection marker that is present along with *Prgef-1::gfp–dsRNA* (Figs. 1, 2*B*, 4, S1, and S6–S9). The DNA for *Prgef-1::gfp–dsRNA* in transgenes was detected by PCR using the primers GACTCAAGGAGGGAGAAGAG and GAGAGACCACATGGTCCTTC. A fragment of the *rrf-1* gene was amplified as a control by using the primers TGCCATCGCAGATAGTCC, TGGAAGCAGCTAGGAACAG, and CCGTGACAACAGACATTCAATC (Fig. 2*B*).

**Feeding RNAi.** Worms that were 24 h past the L4 stage were singled onto RNAi plates [NG agar plates supplemented with 1 mM IPTG (Omega) and 25 μg/mL carbenicillin (MP Biochemicals)] with 5 μL of *Escherichia coli* OP50. Twenty-four hours later, once eggs had been laid (typically, all OP50 was consumed by then), the parent worm was picked off the plate, and progeny were fed bacteria with a plasmid expressing *gfp*–dsRNA or with a control plasmid (L4440). For inherited silencing in somatic cells, 3 d later, gravid adults were treated with bleach (0.6% NaOCl and 1.5 M NaOH), and the silencing in progeny, which were protected by their egg shells, was measured when they reached the L4 stage by counting the number of GFP-positive gut nuclei (Fig. 4*C*) (adapted from ref. 5). For silencing in the germline, 2 d later, the germlines of L4-staged animals were imaged (Fig. S5).

**Quantification of Silencing by Imaging.** The silencing of GFP expressed from single-copy transgenes *oxSi221* (*Peft-3::gfp*) or *oxSi487* (*Pmex-5::gfp*) in different genetic backgrounds was compared by imaging L4-staged animals under nonsaturating conditions for the brightest strain being compared using a Nikon AZ100 microscope and a Photometrics Cool SNAP $HQ^2$ camera. When the extent of silencing was measured as a single proportion, 95% confidence intervals and *P* values for comparison of two proportions were calculated as described (3). For Fig. 1*B*, a Leica SP5X confocal microscope was used to measure GFP expression. All images being compared were adjusted identically by using Adobe Photoshop for display.

For Fig. 4*A*, GFP silencing in gut nuclei was measured by imaging L4-staged animals using a Nikon AZ100 microscope

under nonsaturating conditions and counting the number of GFP-positive gut nuclei that were above a fixed threshold of brightness. For all other figures, GFP silencing in gut nuclei was measured by counting the number of bright GFP-positive nuclei at a fixed magnification on an Olympus MVX10 fluorescent microscope. Comparison of this counting with measurements of fluorescence intensity (using Nikon AZ100 microscope and NIS Elements software) revealed that false calling of a GFP-positive nucleus as per the conservative criterion described in Fig. S6 occurred at most for one nucleus per animal. To measure fluorescence intensity in Fig. S6, an L4-staged worm was mounted on a slide after paralyzing the worm by using 3 mM levamisole (Sigma-Aldrich; catalog no. 196142). Fluorescence intensity in each nucleus of the worm was calculated by using the formula $A_n(I_n - I_b)$, where $A_n$ = area of the nucleus; $I_n$ = mean intensity within the nucleus; and $I_b$ = mean intensity in an area of the slide outside the worm.

**Semiquantitative RT-PCR.** RNA from each strain was isolated by solubilizing 10 L4-staged animals in TRIzol (Ambion, catalog no. 15596-018) using three freeze–thaw cycles, followed by two cycles of chloroform extraction, and a final precipitation in 100% isopropanol with 10 μg of glycogen (Invitrogen, catalog no. 10814-010; Ambion, catalog no. AM9510) as a carrier. The RNA pellet was washed twice in 75% ethanol, resuspended in diethylpyrocarbonate-treated water, and treated with DNase I (New England Biolabs, catalog no. M0303S) for 60 min at 37 °C. The DNase was heat-inactivated for 10 min at 75 °C, and the concentration of RNA was measured (NanoVue). Within each biological repeat of the experiment, the same amount of total RNA was used as template for reverse transcription with SuperScript III (Invitrogen, catalog no. 18080-085) by using gene-specific primers designed to reverse-transcribe the sense strand (AGGGCAGATTGTGTGGACAG for *gfp* and TCGTCTTCGGCAGTTGCTTC for *tbb-2*). The resulting cDNA was used as a template for PCR (27 cycles for *sur-5::gfp*, 30 cycles for *Pmex-5::gfp*, and 30 cycles for *tbb-2*) using Taq polymerase and gene-specific primer pairs (AAGAGTGCCATGCCCGAAG and CCATCGCCAATTGGAGTATT for *gfp* and GACGAGCAAATGCTCAACG and TTCGGTGAACTCCATCTCG for *tbb-2*). Intensity of each band was calculated by using ImageJ (NIH) and the formula $A(I - I_b)$, where $A$ = area of the band; $I$ = mean intensity within the band; and $I_b$ = mean intensity in an area of the gel just above the band. Pictures of the gels were linearly adjusted for display by using Adobe Photoshop without loss of data.

**Genetic Crosses.** Males with an extrachromosomal array were generated for each cross in Fig. 3 by mating hermaphrodites that express the extrachromosomal array in wild-type or mutant backgrounds with wild-type males or corresponding mutant males, respectively. For example, to generate *Ex[gfp–dsRNA]; sid-1(−)* males, *Ex[gfp–dsRNA]; sid-1(−)* hermaphrodites were mated with *sid-1(−)* males. For all crosses with *Pmex-5::gfp* animals in Fig. 3, *dpy-2(e8)* was used as a linked marker to identify the homozygosity of *Pmex-5::gfp*. Only 3% (6/200) of the Dpy progeny of *Pmex-5::gfp*/+ *dpy-2(e8)*/+ double-heterozygous parents were not homozygous for the *Pmex-5::gfp* transgene (determined by Samual Allgood).


1. Jose AM, Garcia GA, Hunter CP (2011) Two classes of silencing RNAs move between *Caenorhabditis elegans* tissues. *Nat Struct Mol Biol* 18(11):1184–1188.
2. Mello CC, Kramer JM, Stinchcomb D, Ambros V (1991) Efficient gene transfer in *C. elegans*: Extrachromosomal maintenance and integration of transforming sequences. *EMBO J* 10(12):3959–3970.
3. Jose AM, Smith JJ, Hunter CP (2009) Export of RNA silencing from *C. elegans* tissues does not require the RNA channel SID-1. *Proc Natl Acad Sci USA* 106(7):2283–2288.
4. Frøkjær-Jensen C, Davis MW, Ailion M, Jorgensen EM (2012) Improved Mos1-mediated transgenesis in *C. elegans*. *Nat Methods* 9(2):117–118.
5. Burton NO, Burkhart KB, Kennedy S (2011) Nuclear RNAi maintains heritable gene silencing in *Caenorhabditis elegans*. *Proc Natl Acad Sci USA* 108(49):19683–19688.


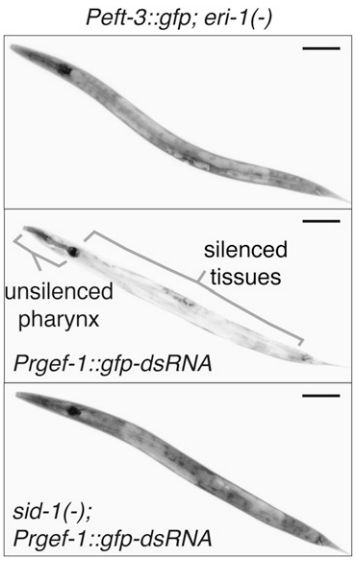


**Fig. S1.** Silencing by neuronal mobile RNAs is dependent on SID-1 even in an enhanced RNAi background. Representative L4-staged animals that express GFP (black) in all tissues (*Peft-3::gfp*) in an *eri-1(–)* (*Top*) background and animals that in addition express dsRNA in neurons against *gfp* (*Prgef-1::gfp–dsRNA*) in *eri-1(–)* (*Middle*) or *eri-1(–); sid-1(–)* (*Bottom*) backgrounds are shown. Detectable silencing was observed in 100% of *eri-1(–)* animals ($n$ = 90) and 0% of *eri-1(–); sid-1(–)* animals ($n$ = 88). Silenced tissues and unsilenced pharynx are indicated (*Middle*). (Scale bars, 50 μm.)

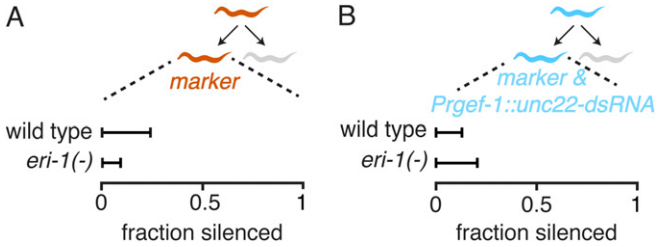


**Fig. S2.** Silencing in the germline by neuronal mobile RNAs is sequence-specific. (*A*) A repetitive transgene that lacks homology to *gfp* sequence does not cause silencing of GFP expression in the germline even in an *eri-1(–)* background. The proportions of animals that showed silencing of GFP expression in the germline were determined for *Pmex-5::gfp* or *Pmex-5::gfp; eri-1(–)* animals that express the co-injection marker alone (orange worm). (*B*) Neuronal mobile RNAs against the somatic gene *unc-22* do not cause silencing of GFP expression in the germline. The proportions of animals that showed silencing of GFP expression in the germline were determined for *Pmex-5::gfp* or *Pmex-5::gfp; eri-1(–)* animals that express neuronal *unc-22 dsRNA* (cyan worm). Error bars indicate 95% CI and $n > 20$ L4-staged animals.

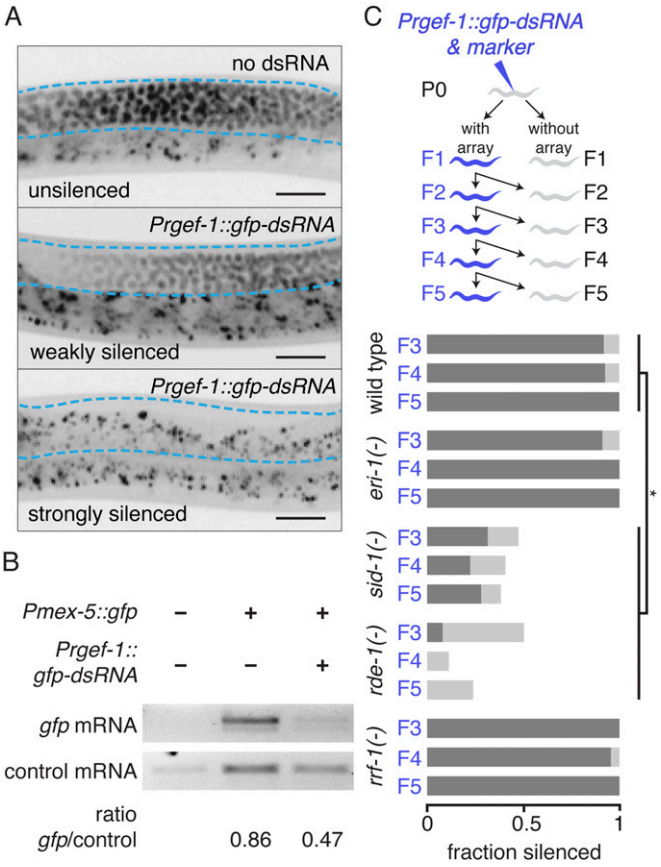


**Fig. S3.** Potent silencing by transgenes that express neuronal dsRNA requires neuronal mobile RNAs even when the transgenes are generated in animals that express the germline target gene. (*A*) Extent of germline silencing due to neuronal mobile RNAs can vary. Representative L4-staged animals that express GFP (black) from the *Pmex-5::gfp* transgene in the germline (outlined in cyan) (*Top*) and animals that in addition express dsRNA in neurons against *gfp* (*Prgef-1::gfp–dsRNA*) but show weak (*Middle*) or strong (*Bottom*) silencing are shown. Because of the long exposure time required for these images, variable and irregular autofluorescence of the gut granules was also detected. (Scale bars, 10 μm.) (*B*) Loss of GFP fluorescence in the germline is due to reduction in levels of *gfp* mRNA. Semiquantitative RT-PCR was used to detect *gfp* mRNA and *tbb-2* mRNA (control) in wild-type animals, *Pmex-5::gfp* animals, and *Pmex-5::gfp* animals that in addition express *Prgef-1::gfp–dsRNA*. The intensity of the *gfp* band was normalized to that of the *tbb-2* band in each sample. (*C*) Silencing of GFP expression in the germline by dsRNA expressed in neurons requires SID-1 and RDE-1, but not ERI-1 or RRF-1. Wild-type, *eri-1(–)*, *sid-1(–)*, *rde-1(–)*, or *rrf-1(–)* animals that express *Pmex-5::gfp* (P0 generation) were injected with constructs to express *Prgef-1::gfp–dsRNA* along with a co-injection marker (*Pmyo-2::DsRed*). For each genetic background, the proportions of worms with fluorescence from the co-injection marker (blue worm) that showed either strong (dark gray bars; as shown in *A*, *Bottom*) or weak (light gray bars; as shown in *A*, *Middle*) silencing of GFP expression in the germline were determined in the F3 ($n$ = 11–24 L4-staged animals), F4 ($n$ = 18–39 L4-staged animals), and F5 ($n$ = 17–29 L4-staged animals) generations. *$P < 0.05$ (Student's $t$ test).

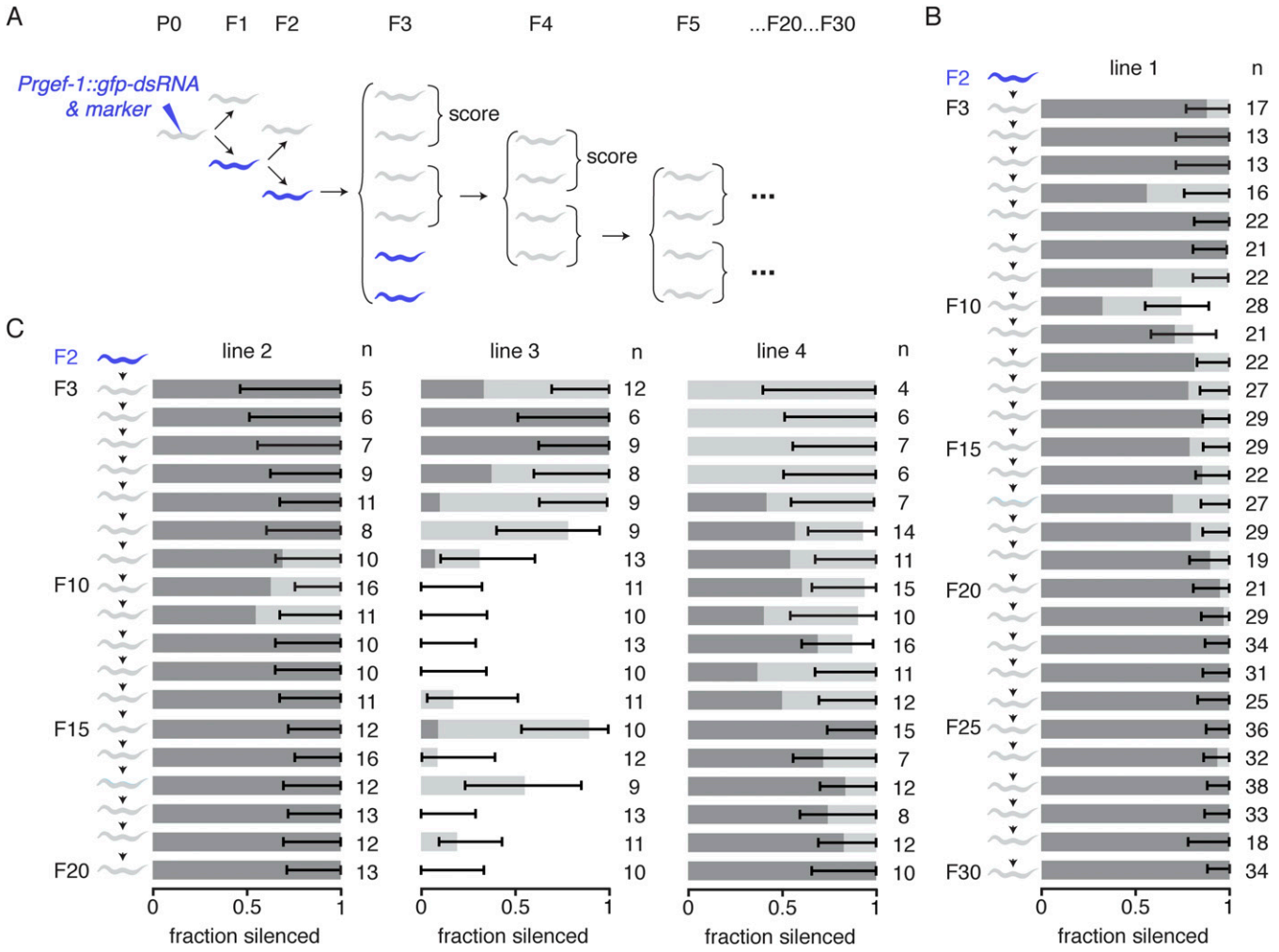


**Fig. S4.** Inherited silencing in the germline can persist for many generations after the source of neuronal mobile RNAs is lost. (*A*) Schematic of the assay for transgenerational silencing by neuronal mobile RNAs. *Pmex-5::gfp* animals (P0) were injected with constructs to express neuronal mobile RNA (*Prgef-1::gfp–dsRNA*) along with a co-injection marker (*Pmyo-2::DsRed*) to generate F2 transgenic lines (blue worm). F3 progeny and their descendants that lost the extrachromosomal array but were derived from F2 transgenic parents were scored for silencing by imaging the germline to detect the silencing of GFP. At each generation, the siblings of the scored animals were propagated to obtain the next generation. (*B* and *C*) The persistence of transgenerational silencing varies from one transgenic line to another. The proportions of animals that lack fluorescence from the co-injection marker (gray worm) but that show either strong (dark gray bar) or weak (light gray bar) silencing in the F3 generation and in successive generations (F4–F30 in *B* and F4–F20 in *C*) were determined for four independent transgenic lines (lines 1–4). Error bars indicate 95% CI, and *n* indicates number of L4-staged animals scored at each generation. Dark gray bars and light gray bars are as in Fig. S3C.

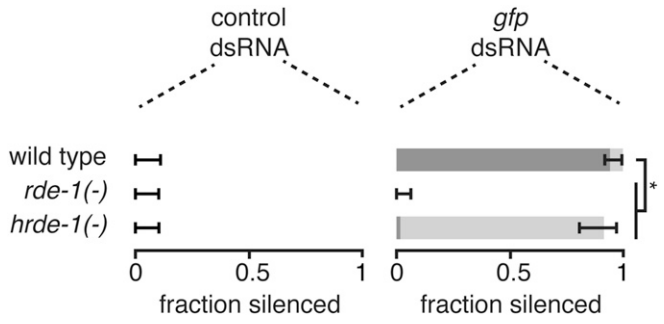


**Fig. S5.** Ingested dsRNAs can silence a gene within the germline independent of HRDE-1. Wild-type, *rde-1(–)*, or *hrde-1(–)* animals that all express *Pmex-5::gfp* were exposed for one generation to bacteria that have either the control L4440 plasmid (control dsRNA) or a plasmid that encodes dsRNA against *gfp* (*gfp* dsRNA) and silencing of GFP expression in the germline was measured. Error bars indicate 95% CI. **P* < 0.05. *n* > 35 L4-staged animals. Dark gray bars and light gray bars are as in Fig. S3C.

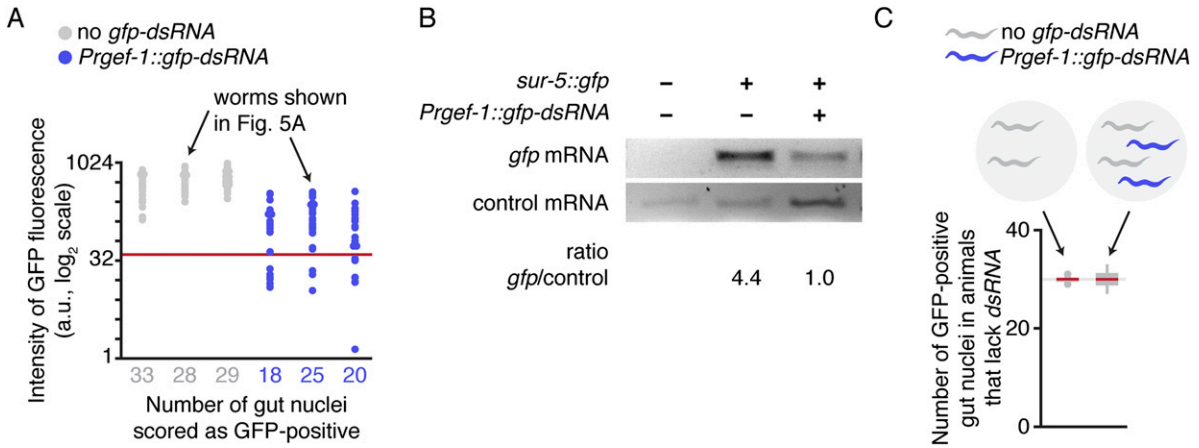


**Fig. S6.** Silencing by neuronal mobile RNAs against *gfp* reduces GFP fluorescence as well as *gfp* mRNA levels and is due to transport of mobile RNAs from neurons to other cells in animals that express dsRNA. (*A*) Nuclei counted as showing GFP silencing have several fold lower intensity of GFP fluorescence than even the dimmest nucleus in animals that do not show silencing. Intensity of GFP fluorescence in each gut nucleus of *sur-5::gfp* animals (no *gfp–dsRNA*, gray) or *sur-5::gfp* animals that express neuronal dsRNA (*Prgef-1::gfp–dsRNA*; blue) was measured and compared with the number of nuclei counted as not silenced for each worm (indicated along the *x* axis). Red line indicates threshold of expression below which a nucleus was scored as silenced in Figs. 4, 5*B*, S6*C*, and S7–S9. (*B*) Silencing of somatic GFP by neuronal mobile RNAs is due to reduction in mRNA levels. Semiquantitative RT-PCR was used to detect *gfp* mRNA and *tbb-2* mRNA (control) in wild-type animals, *sur-5::gfp* animals, and *sur-5::gfp* animals that in addition have *Prgef-1::gfp–dsRNA*. The intensity of the *gfp* band was normalized to that of the *tbb-2* band in each sample. (*C*) Animals that express neuronal mobile RNAs do not cause silencing in animals that lack neuronal mobile RNAs when grown together. The numbers of GFP-positive gut nuclei in animals that express *sur-5::gfp* were determined after growing the strain alone or after growing the strain for 4 d along with animals that contain both *Prgef-1::gfp-dsRNA* (marked with a dominant Rol defect) and *sur-5::gfp*. Gray line and red bar are as in Fig. 4*B*, and $n > 25$ L4-staged animals.

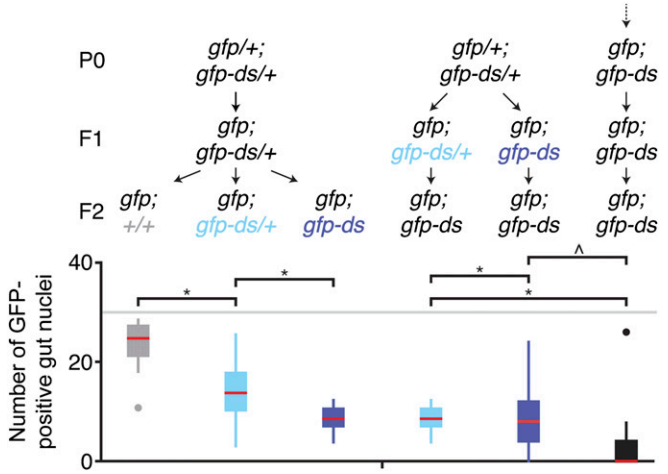


**Fig. S7.** Changes in parental mobile RNA silencing are correlated with small changes in mobile RNA silencing in progeny. Extent of RNA silencing in parents was varied, and inheritance of silencing was measured by comparing progeny of identical genotype in an *eri-1(–)* background. (*Left*) Dosage of dsRNA transgene in neurons against *gfp* dictates the level of silencing observed. Numbers of GFP-positive gut nuclei were counted in animals that either lack (gray) or that have one (cyan) or two copies (blue) of *Prgef-1::gfp–dsRNA* (*gfp–ds*) transgene. (*Right*) Increased mobile RNA silencing in parents is correlated with a small increase in mobile RNA silencing in progeny. Numbers of GFP-expressing gut nuclei were counted in animals that all expressed *Prgef-1::gfp–dsRNA* (*gfp–ds*) but that were progeny of parents that expressed one copy of *Prgef-1::gfp–dsRNA* (cyan), two copies of *Prgef-1::gfp–dsRNA* for one generation (blue), or two copies of *Prgef-1::gfp–dsRNA* for many generations (black). Gray line, red bar, and asterisks are as in Fig. 4*B*. ^$P = 0.054$. $n > 15$ L4-staged animals. These results are consistent with a small increase in silencing by mobile RNAs due to parental or ancestral silencing signals.

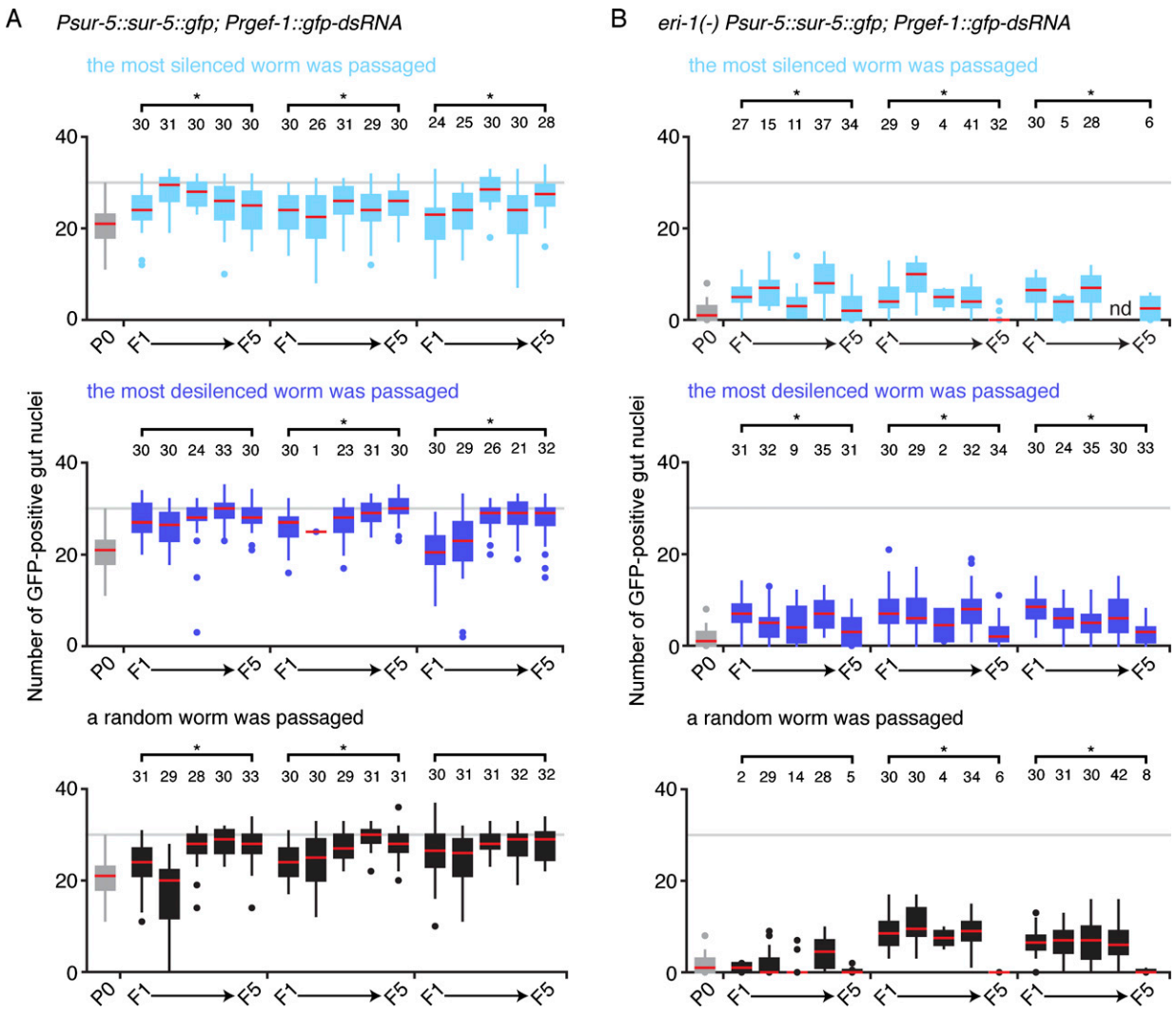


**Fig. S8.** Neuronal mobile RNAs can show small variations in silencing a somatic gene across generations. Animals that express neuronal mobile RNAs (*Prgef-1::gfp–ds RNA*) in *Psur-5::sur-5::gfp* (*A*) or in *eri-1(–) Psur-5::sur-5::gfp* (*B*) backgrounds were propagated for five generations (F1–F5) in triplicate by selecting at each generation the most silenced animal (cyan), the most desilenced animal (blue), or a random animal (black) from a starting population of animals (P0) and the numbers of GFP-expressing gut nuclei in L4-staged animals of each generation were counted. Gray line, red bar, and asterisks are as in Fig. 4*B*. The number of animals assayed in each generation varied from 1 to 42 and are indicated above each box plot.

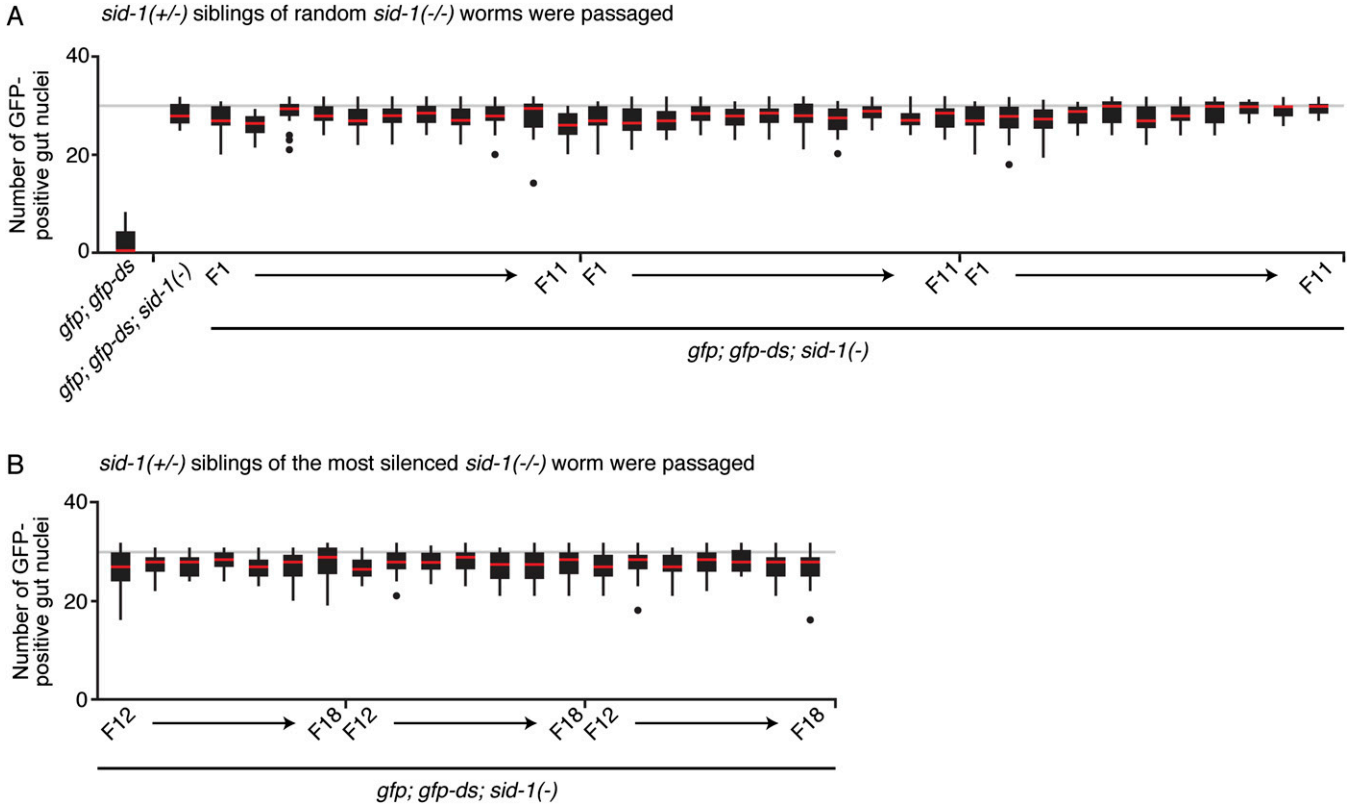


**Fig. S9.** SID-1 is required for silencing by neuronal mobile RNAs even after 17 generations of ancestral silencing. The numbers of GFP-positive gut nuclei were counted in animals that express neuronal mobile RNAs (*gfp–ds*) and nuclear-localized GFP in all somatic tissues (*gfp*) in an *eri-1(–)* background (*gfp; gfp–ds*) or in an *eri-1(–); sid-1(–)* background [*gfp; gfp–ds; sid-1(–)*]. By using the schematic described in Fig. 4*E*, *sid-1(–/–)* animals were generated after different numbers of generations of *sid-1(+/–)* animals that all had *gfp* and *gfp–ds*. The numbers of GFP-positive gut nuclei were counted in L4-staged *sid-1(–/–)* animals of each generation when *sid-1(+/–)* heterozygous siblings were passaged in triplicate without any selection for 11 generations (*A*) or when *sid-1(+/–)* siblings of the most silenced *sid-1(–/–)* animal were passaged in triplicate for seven more generations (*B*). Gray line, *n*, and red bars are as in Fig. 4*B*.